

ASSESSMENT OF FLEXURAL BEHAVIOUR OF HIGH-STRENGTH CONCRETE REINFORCED WITH REBARS AND STEEL FIBRES

Torsten Müller (1), Hubertus Kieslich (1) and Klaus Holschemacher (1)

(1) Leipzig University of Applied Sciences, Germany

Abstract

In this paper the results of a research program focused on the influence of steel fibre types and content as well as different bar reinforcements on flexural tensile strength, fracture behaviour and workability of steel bar reinforced high-strength steel fibre reinforced concrete (HSSFRC) are demonstrated. The parameters which were investigated are in detail the influence of fibre geometry (straight with end hooks, corrugated), tensile strength of fibres (1100 N/mm², 1900 N/mm²) and different steel bar reinforcements (without rebars, 2 Ø 6 mm, 2 Ø 12 mm) in combination with diverse fibre contents (from 20 to 60 kg/m³). The basis for evaluating the efficiency of the different steel fibres together with the reinforcing steel are force-displacement curves of SFRC beams, gained in four point bending tests. Thereby, the average cube concrete compressive strength ranges between 85 and 102 N/mm². According to the German guideline of “Steel Fibre Reinforced Concrete” [1], beams of 150 x 150 mm cross section with a length of 700 mm were used as specimens.

Résumé

Cet article présente les résultats d’une recherche sur l’influence de la teneur et du type de fibres d’acier ainsi que différents ferraillements sur la résistance en flexion, la rupture et l’ouvrabilité du béton armé renforcé de fibres métalliques à haute résistance. Les paramètres étudiés sont la géométrie des fibres (droites à crochets, ondulées), la résistance en traction des fibres (1100 N/mm², 1900 N/mm²) et différents taux de ferraillement (non armé, 2 Ø 6 mm, 2 Ø 12 mm) combinés à différents taux de fibres (de 20 à 60 kg/m³). L’évaluation de l’efficacité des différents renforts de fibres et armatures se base sur les courbes force-déplacement de poutres testées en flexion 4 points. La résistance moyenne en compression du béton varie de 85 à 102 MPa. Conformément aux recommandations allemandes sur les bétons renforcés de fibres d’acier [1], les corps d’épreuve utilisés sont des poutres de 700 mm de long et de section 150 x 150 mm.

1. INTRODUCTION

In the German Guideline on “Steel Fibre Reinforced Concrete” [1] from the German Committee for Reinforced Concrete (DAfStb), some areas of the concrete construction are not

covered, due to limited experimental data. Lightweight concretes (LWC) as well as high strength concretes (HSC) are generally excluded. Hence, the current research is aimed to study the load bearing and deformation behaviour of high strength steel fibre reinforced concrete (HSSFRC) with and without conventional bar reinforcement.

2. EXPERIMENTAL PROGRAM

The experimental program includes investigations on the influence of geometry and tensile strength of fibres as well as effects of different bar reinforcements. The applied fibre contents (FC) were 20, 30, 40 and 60 kg/m³. The tests were carried out according to the recommendations of the German Concrete Association for SFRC [2] on small beams (15 x 15 x 70 cm).

2.1 Materials and mixture proportions

Four different fibre types were selected:

- two straight fibres types with end hooks (F1 and F2) and
- two corrugated fibre types (F3 and F4).

Thereby, the fibre variants F1 and F3 represent normal strength fibres, whereas F2 and F4 can be characterized as high strength steel fibres. The properties of the selected steel fibre types are shown in Table 1. In all cases the modulus of elasticity averages 200,000 N/mm².

Table 1: Overview of investigated steel fibre types

Description		F1	F2	F3	F4
View					
Parameters		Geometry			
Surface		plane			
Cross-section		circular			
Shape		straight		corrugated	
Anchorage		hooked ends		continuous	
Parameters	Units	Values			
l_f	[mm]	50			
d_f	[mm]	1			
λ	[mm]	50			
f_t	[N/mm ²]	1100	1900	1100	2000
$f_t^{1)}$	[N/mm ²]	1189	1762	925	1873
n_f	[kg ⁻¹]	3183	3188	2903	3642
¹⁾ experimentally determined fibre tensile strength (average for 10 fibres)					

The abbreviations mentioned above are detailed as follows:

l_f fibre length, d_f fibre diameter, $\lambda = l_f/d_f$ aspect-ratio,
 f_t fibre tensile strength, n_f number of fibres per kg.

The following additional materials were used:

- composite Portland cement (with portions of granulated slag and limestone between 6 and 20 % with a density of 3.05 kg/dm³ and a fineness of 4660 cm²/g),
- fly ash (with specific gravity of 2.3 kg/dm³ and grain sizes between 2 and 290 μ m),

- polycarboxylic ether - based superplasticizer (with a density of 1.07 kg/dm³),
- long-term retarder, based on phosphonic acid (with a density of 1.17 kg/dm³),
- locally available natural sand (with a fraction size of 0 to 2 mm used as fine aggregate),
- two different types of gravel (with a fraction size of 2 to 8 mm and 8 to 16 mm).

Sand and gravel had a specific gravity of 2.65 kg/dm³. The applied grain size distribution of aggregates ranged between A16 and B16, according to [3]. Altogether 17 concrete mixtures were fabricated for casting the specimens used in further tests. The reference concrete composition (R) is shown in Table 2. By applying different fibre contents, the amounts of superplasticizer and retarder were adapted up to a maximum value of 12.4 kg/m³ (superplasticizer) and 2.4 kg/m³ (retarder). Based on this reference concrete mixture, the HSSFRC were made for different fibre amounts (20, 30, 40 and 60 kg/m³) and fibres types F1 to F3. For the fibre variant F4 only 30 and 60 kg/m³ were chosen. All concrete mixtures were mixed in a 0.5 m³ single-shaft compulsory mixer. The calculated volume of each mixture was 0.380 m³. To reduce the influence of the aggregates' moisture on concrete properties, dried aggregates were used for all mixtures.

Table 2: Concrete mix-proportions

Components		Composition R	Unit
Cement	c	400.0	kg/m ³
Total water	w	132.0	kg/m ³
w/c ratio		0.330	-
Additives	Steel fibres	0	kg/m ³
	Fly ash (FA)	100.0	kg/m ³
w/(c+FA) ratio		0.264	-
Admixtures	Superplasticizer	10.0	kg/m ³
	Retarder	0.8	kg/m ³
Aggregates	0/2 sand	39.0	%
	2/8 gravel	25.0	%
	8/16 gravel	36.0	%

2.2 Testing fresh mixture's properties

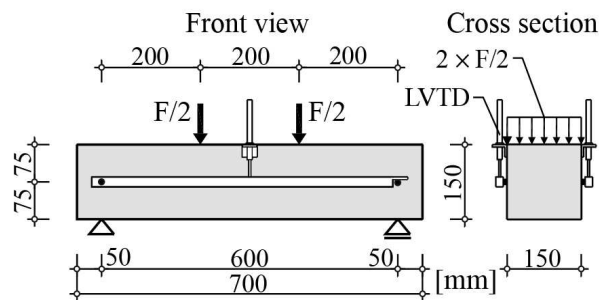


Figure 1: Experimental setup of the four point bending test

Following [4], one workability test (slump test) was carried out for each HSC and HSSFRC mixture in a lapse of 5 minutes after finishing mixing. The target slump (a_5) was between 56 and 62 cm, corresponding to [4]. The concrete compressive and splitting tensile

strengths were measured for six cubes with an edge length of 150 mm for each fibre type and content. Additionally, the elasticity modulus was investigated on three cylinders with a height of 30 cm and a diameter of 15 cm. Finally, four-point bending tests were carried out to investigate the post-cracking behaviour. For this reason HSC and HSSFRC beams with a cross section of 150 x 150 mm and a length of 700 mm were casted. A scheme of the test setup is shown in Figure 1. According to [1, 2], the beams were loaded orthogonal to the casting direction. The load was controlled using a displacement method with a rate of 0.2 mm/min. The deflection was recorded by two LVDTs (one on each side of the beam).

Table 3: Number of tested beams per series

FC kg/m ³	without steel bars					B500 – 2 Ø 6 mm						B500 – 2 Ø 12 mm				
	R1	F1	F2	F3	F4	R1	R2	F1	F2	F3	F4	R1	F1	F2	F3	F3*
0	6					6	6					6				
20		6	6	6				6	6	6			6	6	6	9
30		6	6	6	3			6	6	6	3		6	6	6	
40		6	6	6				6	6	6			6	6	6	
60		6	6	6	3			6	6	6	3		6	6	6	

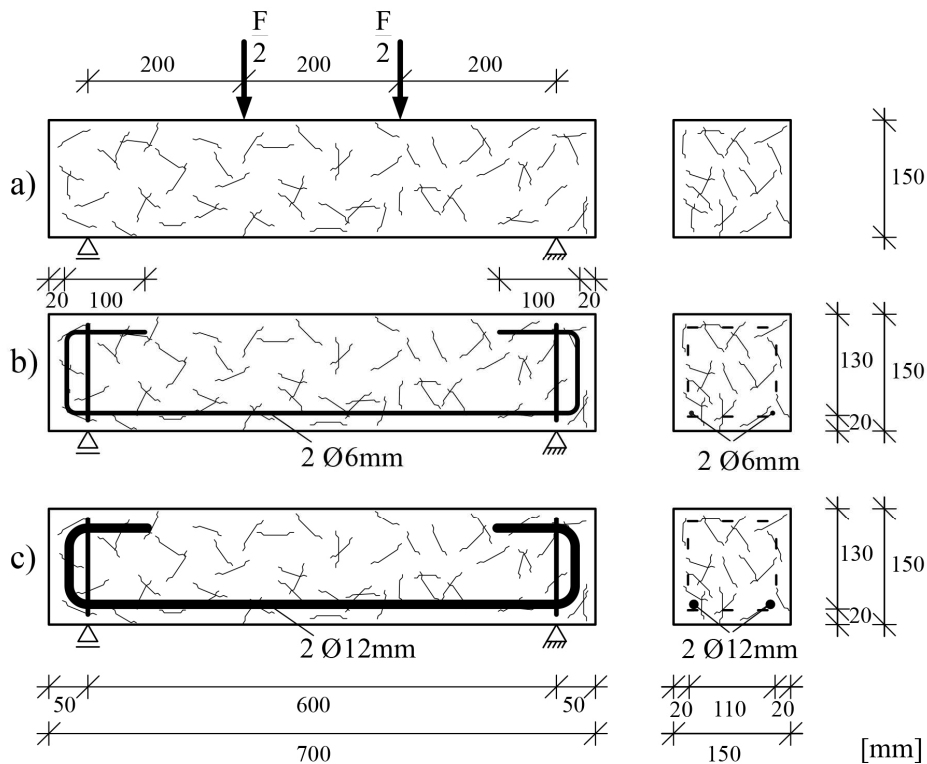


Figure 2: Test specimens: (a) without bar reinforcement; (b) with 2 Ø 6 mm; (c) with 2 Ø 12 mm

In total 261 beams were tested. The units of tested beams per series are summarized in Table 3. In Figure 2 an overview of the used types of longitudinal steel bar reinforcements of the tested beams is given. For each fibre content 18 specimens were casted normally. Among

them 12 were provided with two different steel bar reinforcement ratios (2 Ø 6 mm with 0.25 %, 2 Ø 12 mm with 1.0 %) and 6 beams without steel bar reinforcement. Longitudinal tensile reinforcement had hooks at the beam ends to ensure adequate anchorage. Additionally, stirrups (Ø 6 mm) were attached at the supports to hold the bar reinforcement. The steel bars were characterized by specified yield strength of 500 N/mm² (B500 according to [5]). The hardened properties of the mixtures were tested 28 days after casting.

3. EXPERIMENTAL RESULTS

3.1 Properties of fresh concrete

HSC has a low water-binder ratio. Hence, the concrete mixtures were characterized by high viscosity, resulting in problematic workability. However, during the tests a uniform distribution and a random orientation of fibres, without any signs of balling or clustering, were observed. Table 4 presents the slump test results (a_5) as well as concrete and ambient temperatures (T_C , T_A) of different HSC and HSSFRC mixtures. As it was mentioned above the slump should be between 56 and 62 cm. In most cases this requirement was satisfied.

Table 4: Overview of determined fresh concrete properties

B500 – 2 x Ø			FC	FT	a_5	T_C	T_A
[mm]			[kg/m ³]	[-]	[cm]	[°C]	[°C]
0	6	12	0	R1	62	28.2	19.0
6				R2	40	16.3	-3.0
0	6	12	20	F1	63	20.1	3.5
0	6	12		F2	57	21.3	6.3
0	6	12		F3	62	25.2	18.0
12				F3*	58	26.6	18.8
0	6	12	30	F1	59	21.5	7.5
0	6	12		F2	56	20.4	4.1
0	6	12		F3	59	26.5	18.2
0	6			F4	42	11.1	-1.2
0	6	12	40	F1	56	21.9	4.2
0	6	12		F2	56	20.5	4.8
0	6	12		F3	65	33.6	26.8
0	6	12	60	F1	57	19.8	2.5
0	6	12		F2	63	22.3	11.0
0	6	12		F3	62	29.0	23.0
0	6			F4	40	11.7	-2.7

3.2 Properties of hardened concrete

In this section the experimental results of compressive strength, splitting tensile strength, modulus of elasticity, concrete density (compare Table 5) and load bearing behaviour of beams are presented. The compressive strength is required for classification of concrete according to the strength classes. The splitting tensile strength is important for indirect determination of concrete tensile strength. The investigation of load bearing behaviour of

beams allows the determination of concrete bending strength. It is also required for assessment of the post-cracking tensile strength in service and ultimate limit states, as well as for evaluation of the fracture behaviour of concrete and for the determination of fibre segregation and distribution. Average compressive and splitting tensile strengths for specimens with different fibre contents are given in Table 5. Following these results, in average the strength increases as the fibre content becomes higher. The compressive strength for all HSSFRC specimens was higher than for HSC ones. Generally, the splitting tensile strength increases with the raise in fibre content.

Table 5: Overview of determined hardened concrete properties

B500 – 2 x Ø	FC	FT	Compressive strength		Splitting tensile strength		Modulus of elasticity		density
			cube		cube		cylinder		
			$f_{cm,cube}$	s	$f_{ctm,sp}$	s	E_{cm}	s	
[mm]	[kg/m ³]	[-]	[N/mm ²]	[N/mm ²]	[N/mm ²]	[N/mm ²]	[N/mm ²]	[kg/dm ³]	
0 6 12	0	R1	86.1	2.29	4.18	0.22	38438	777	2.41
6		R2	85.3	8.00	4.56	0.36	35692	1065	2.35
0 6 12	20	F1	86.8	6.44	5.12	0.26	43106	1143	2.43
0 6 12		F2	91.4	3.74	4.86	0.27	41383	1860	2.43
0 6 12		F3	86.2	5.02	4.84	0.05	40327	1027	2.42
12		F3*	94.5	1.28	5.24	0.40	41879	1142	2.43
0 6 12	30	F1	90.8	4.15	5.01	0.44	40428	935	2.44
0 6 12		F2	86.2	2.24	5.42	0.22	39938	1450	2.43
0 6 12		F3	88.5	1.35	5.11	0.28	42598	1010	2.44
0 6		F4	86.4	1.62	4.39	0.83	36744	1221	2.38
0 6 12	40	F1	91.1	1.33	5.63	0.23	41238	2316	2.44
0 6 12		F2	91.7	1.81	5.02	0.16	40103	476	2.44
0 6 12		F3	95.4	1.13	4.96	0.48	41686	843	2.43
0 6 12	60	F1	88.2	3.53	6.17	0.85	40307	1271	2.44
0 6 12		F2	102.1	2.98	5.89	0.78	40959	1086	2.46
0 6 12		F3	93.3	1.65	5.10	0.57	43854	1598	2.43
0 6		F4	92.6	3.38	5.29	1.26	38100	1279	2.43

Analysing pre- and post-cracking behaviour is important for design of SFRC members, subjected to bending. According to the modern standard, applied in Germany [1], residual flexural tensile strength is of particular importance. The influence of fibre content and type as well as different bar reinforcement on pre- and post-cracking behaviour of HSC and HSSFRC beams is shown in Figure 2. All specimens demonstrated an increase in the load level in post-cracking range as the fibre content became higher. However, by changing the fibre content from 20 to 60 kg/m³, the load bearing capacity is not tripled, because the relation between the effective fibres and fibre content is nonlinear. For specimens with reinforcing steel 2 Ø 6 mm curves for R1 and R2 (without fibre reinforcement) after the first crack have jumps because additional cracks appeared immediately after the first one has developed. These jumps may be avoided by adding fibres. In specimens without bar reinforcement the load in the post-cracking range decreases with increasing deflection (Table 6 a to d). For beams with bar reinforcement the load increases after the crack formation.

Table 6: Average load-deflection curves for different fibre types (F1 to F4) with different fibre contents and bar reinforcement ratios

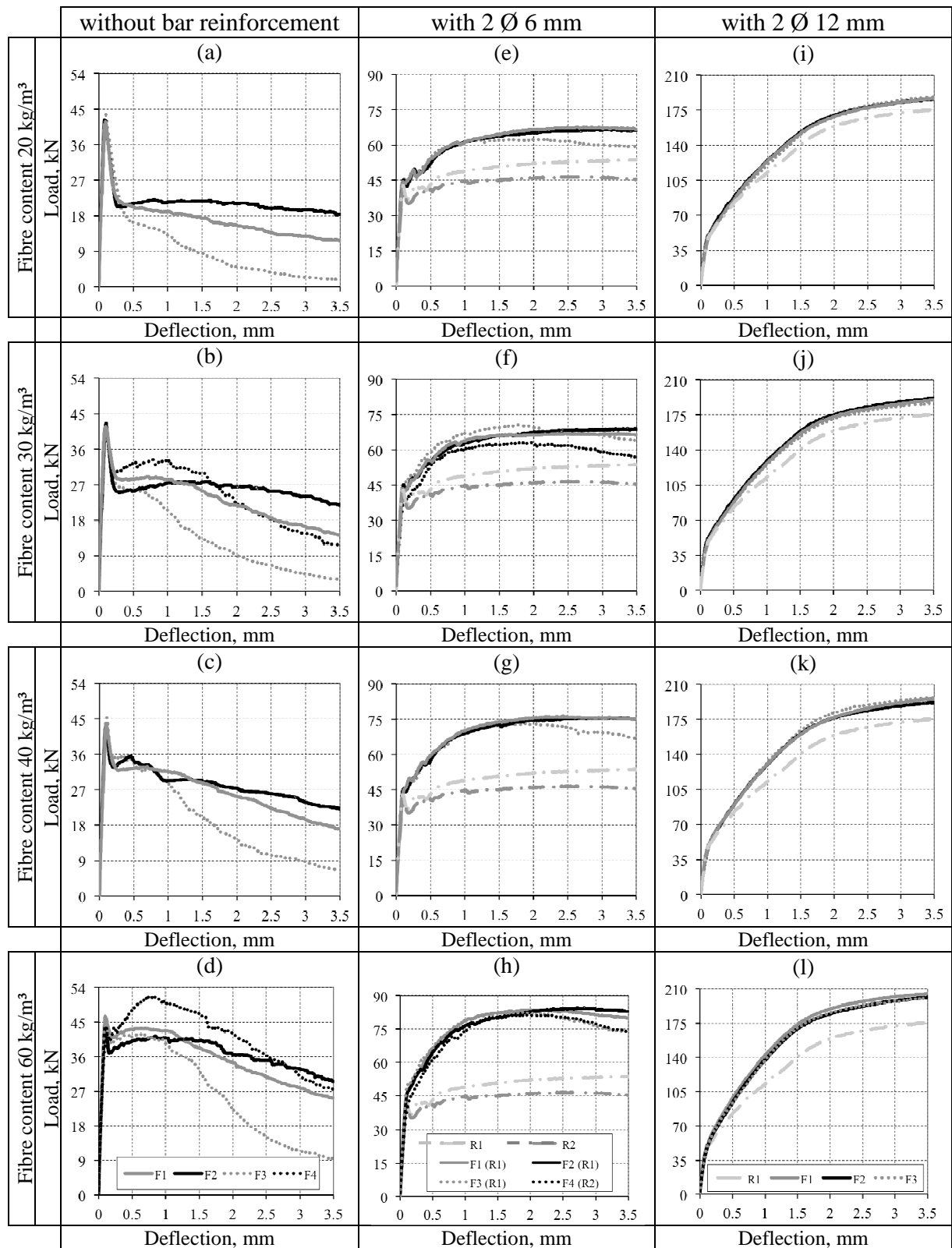
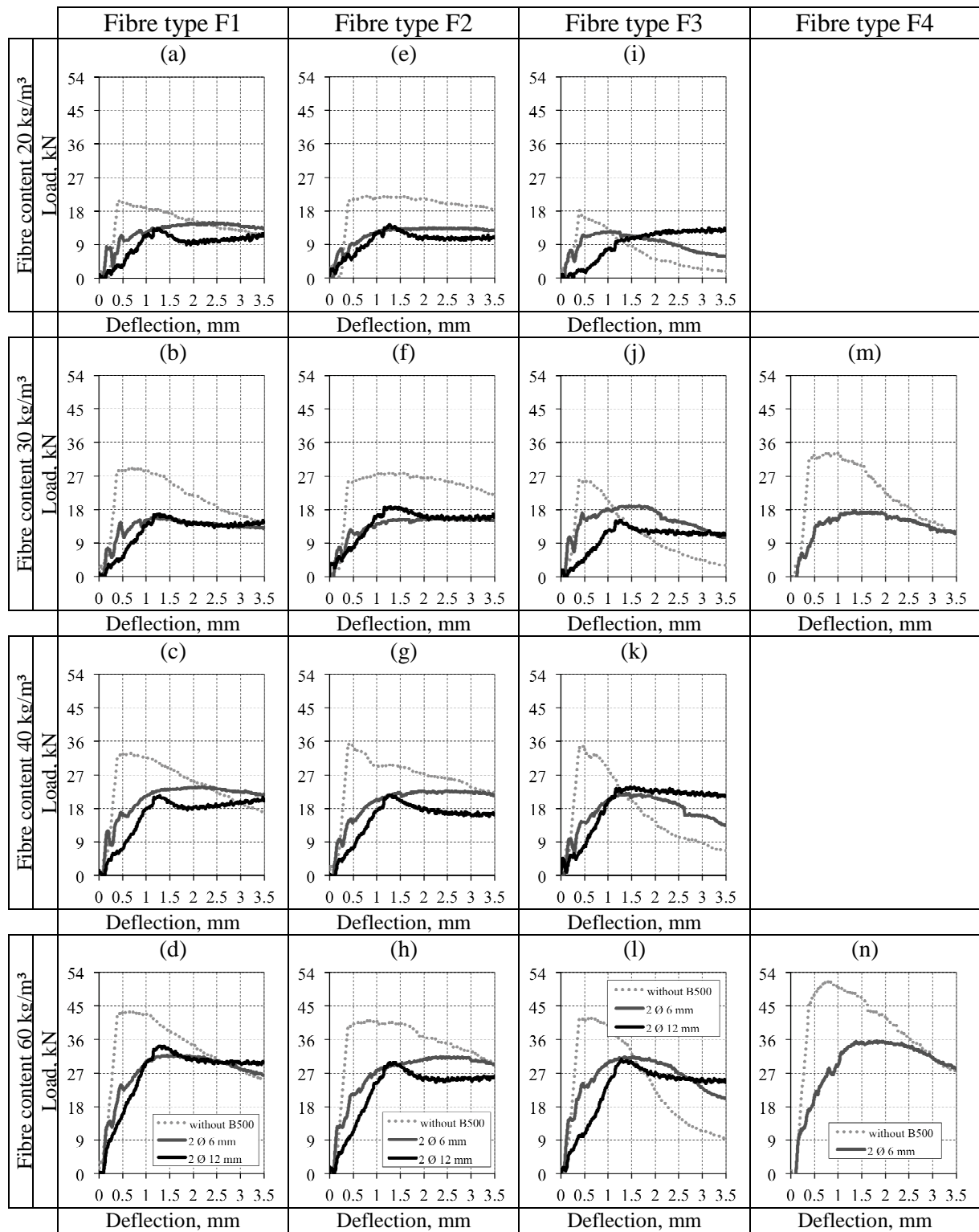


Table 7: Average load-deflection contributions of fibres for different fibre types (a to d – F1, e to h – F2, i to l – F3, m and n – F4) with different fibre contents and bar reinforcement ratios



The increase becomes more evident for higher bar reinforcement ratio. For specimens combined with end anchored fibre types (F1 and F2) and 2 Ø 6 mm the loading rate at 3.5 mm was generally higher, compared to that in specimens with corrugated fibre types (F3 and F4). Regarding specimens with high reinforcement ratio (2 Ø 12 mm), the influence of fibre type is comparatively small. It should be mentioned that the tested beams had different failure modes. The following notations can be used for different failure models: BT, failure in bending, tensile reinforcement bars are failed; BC, failure in bending, concrete in the compressed zone is collapsed; BS, failure in shear.

For example, specimens with a reinforcement ratio of 1 % (2 Ø 12 mm) and none or low fibre contents (0 and 20 kg/m³) failed in BC or BS, and for fibre contents from 40 to 60 kg/m³ primary compression failure (BC) was observed. Specimens with bar reinforcement ratio ≤ 0.25 % (2 Ø 6 mm) failed in bending (BT). Specimens that failed in shear and have not reached a deflection of 3.5 mm have not been included in calculations of average results.

Table 7 presents the contribution of fibres to the load-deflection curves. For specimens without bar reinforcement the force-deflection curves for HSC beams were subtracted from those obtained for HSSFRC ones. For specimens with bar reinforcement the load-deflection curves were generated by subtraction of loads, determined for beams with bar reinforcement without fibres from beams with fibres and longitudinal reinforcement.

Normally, with increasing bar reinforcement ratio, the load bearing capacity of steel fibres will be reduced at low deflections (representing the service ability limit state), due to the fact that multiple cracks appear in HSSFRC beams with reinforcing bars. The bar reinforcement initially absorbed a big percentage of the first crack energy as a result of better bonding between the bars and the matrix, compared to that between the fibres and the matrix. As the deflection increased, multiple cracks were noticed and smaller crack widths in respect to the same deformation were measured, compared to beams with a single crack. Slower crack opening caused a slower but continuous activation of fibres. A stronger rise of the curves was observed for the smaller bar reinforcement ratio, independent of fibre type and content.

Referring to this, up to deformations between 1.0 mm and 1.5 mm, a higher working capacity of fibres was observed for specimens with 2 Ø 6 mm, compared to those with 2 Ø 12 mm, because of a higher activation of the fibres during the load transfer after repeated matrix failure on the basis of lower bond forces of the smaller longitudinal reinforcement. In contrast to the other bar reinforcement ratios a constant load level was observed for the specimens with a bar reinforcement of 2 Ø 12 mm at deflection higher than 2.0 mm.

The average number of fibres in the fractured surface was determined for all tested specimens per series, independent on orientation, position and embedded length of the single fibres. The results are presented in Table 8.

Table 8: Overview of counted number of fibres per series based on test results

FT	average number of counted fibres in the fractured surface based on test results $n_{T,\emptyset}$ [-]			
	Fibre content [kg/m ³]			
	20	30	40	60
F1	44.8	57.9	81.0	124.9
F2	39.1	58.9	80.3	120.1
F3	33.8	57.2	79.3	115.4
F4	-	69.3	-	141.8

Table 9: Calculated number of fibres based on the developed model according to [6, 7]

FT	calculated number of fibres in the fractured surfaces based on model											
	$n_{M,min}$ [-]				$n_{M,\emptyset}$ [-]				$n_{M,max}$ [-]			
	Fibre content [kg/m ³]											
	20	30	40	60	20	30	40	60	20	30	40	60
F1	35.3	63.0	80.6	125.7	43.4	66.8	88.5	131.1	47.3	69.8	90.8	139.5
F2	35.3	63.1	80.7	125.9	43.4	66.9	88.6	131.3	47.3	69.9	90.9	139.7
F3	33.5	58.3	74.7	115.2	40.0	61.6	81.0	118.9	45.0	64.4	86.1	127.3
F4	46.4	71.5	95.5	141.7	50.1	76.5	99.5	150.5	53.1	79.4	105.1	157.9

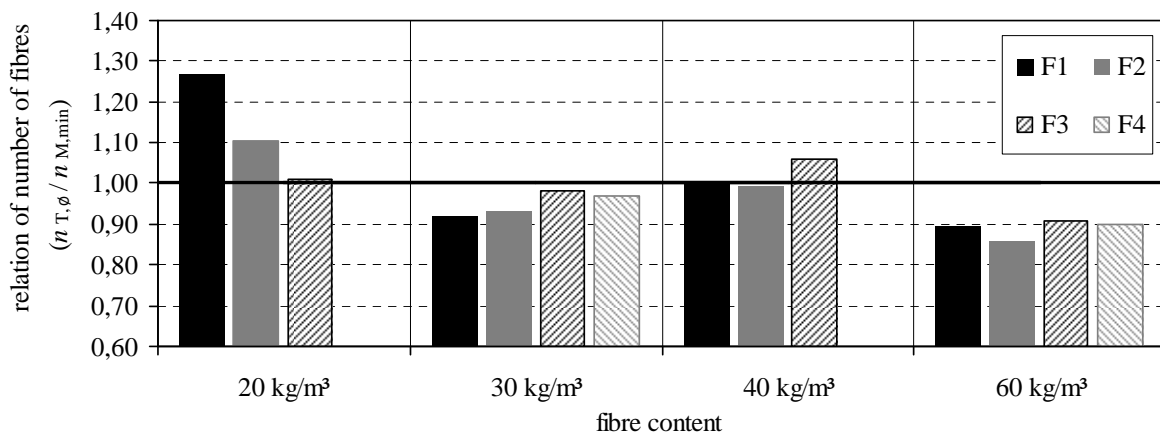


Figure 3: Comparison of number of fibres based on experimental and theoretical results

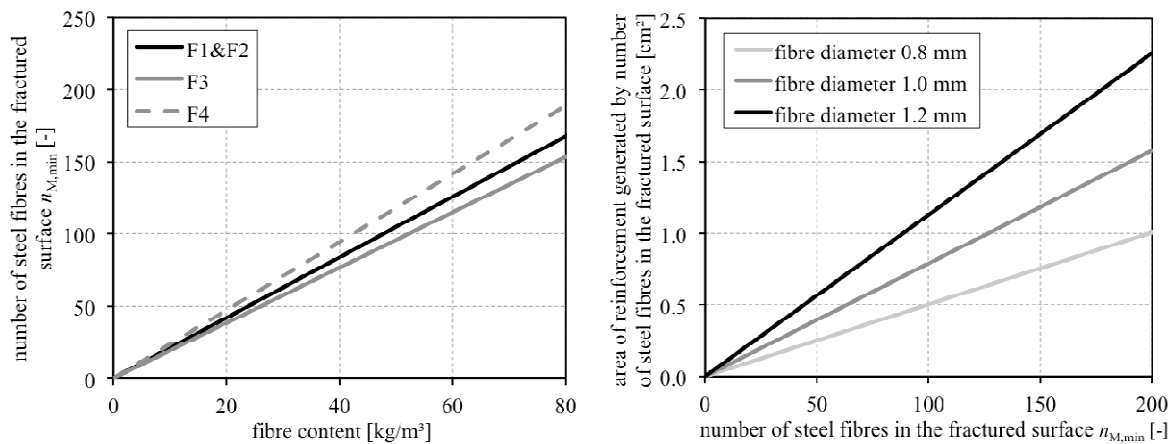


Figure 4: Overview of selected interaction charts

In Table 9 an overview of calculated number of fibres based on the developed model is given. This model was introduced by Mueller in [6, 7]. The minimum, average and maximum values for the investigated fibre types and contents are shown in the table.

Figure 3 presents a comparison of number of fibres, based on experimental and theoretical results, of small beams for different fibre contents. In the diagram the relations of number of fibres resulting from the average values of the experimental results ($n_{T,\emptyset}$) and the minimum

values of the model ($n_{M,min}$) are shown [6, 7]. The value 1.0 characterizes the point reaching accordance between model and experimental results. In general, a good conformity of the model was observed. Regarding the fibre amount of 20 kg/m³ for all fibre types, the average number of fibres in the test ($n_{T,\phi}$) was always higher compared to the minimal number of fibres based on the model ($n_{M,min}$). For this reason the relation is generally over 1.0.

In Figure 4 selected types of interaction charts, based on the fibre model, are shown. In general a linear relation between used fibre content and determined number of fibres in the fractured zone can be assumed (left diagram). The differences in the curves were caused by the existing length and weight of a single fibre. Regarding the right diagram, the area of reinforcement of steel fibres can be derived from the number of fibres in the fractured surface. Thereby, an inference to the effectiveness of fibres in the crack is not considered.

4. CONCLUSIONS

The strength and geometry of fibres have a direct influence on the load bearing capacity of HSSFRC beams without bar reinforcement. Using high strength fibres resulted in a clearly better ductile behaviour and higher load levels in the post cracking range, compared to normal strength ones (for specimen without bar reinforcement). Specimens with high strength fibres had lower number of broken fibres in the failed cross-sections, compared to those with normal strength ones. The use of high-strength fibres in bar reinforced HSC beams is not necessary, as no significant increase in the load bearing capacity, compared to beams with normal-strength fibres, was observed.

In cases of fibre contents of 0 and 20 kg/m³ the specimens, containing bar reinforcement of 1 %, failed in shear or compression. Primary compression failure was observed for specimens with fibre content of 40 kg/m³. For fibre content of 60 kg/m³ the HSC beams with longitudinal reinforcement ratio of 1 % failed in compression only.

In serviceability limit state the highest efficiency of the fibres (specimens without bar reinforcement) was observed for the corrugated high strength fibre type. In ultimate limit state the highest efficiency of the fibres (specimens without bar reinforcement) was observed for the straight high strength fibre type.

If design of steel bar reinforced HSSFRC beams will be based on the test results of specimens without bar reinforcement, the load bearing capacity at serviceability stage (low deformations) will be overestimated, independent of the fibre type. The load level in the range of high deformations, representing the ultimate limit state, will be overestimated for the high strength fibre type.

Normal and high strength corrugated fibre showed higher reserves for design of HSSFRC with bar reinforcement at ultimate limit state compared to fibres with end hooks.

On the basis of the developed model, it is possible to check the used fibre content of a mixture by comparison of the average number of fibres on the fractured surface with the theoretical value resulting from the model.

REFERENCES

- [1] Deutscher Ausschuss für Stahlbeton (DAfStb), Richtlinie Stahlfaserbeton, Beuth Verlag GmbH, Berlin und Köln, December 2010 (in German).
- [2] Deutscher Beton- und Bautechnik-Verein e.V. (Hrsg.), DBV-Merkblatt Stahlfaserbeton, Wiesbaden, October 2001 (in German).

- [3] DIN EN 206-1: Concrete, Part 1: Specification, performance, production and conformity, German version, DIN Deutsches Institut für Normung e.V., July 2001.
- [4] DIN EN 12350-5: Testing fresh concrete, Part 5: Flow table test; German version, DIN Deutsches Institut für Normung e.V., June 2000.
- [5] DIN EN 1992-1-1/National Annex: Design of Concrete Structures. Part 1-1: General rules and rules for buildings. Deutsche Fassung EN 1992-1-1:2005 (D) inklusive Berichtigungen Ber1:2008 (E) und Ber2: 2010 (E) including. Beuth Verlag, Berlin 2011 (in German).
- [6] Mueller, T.; Holschemacher, K.: Model for determination of average number of fibers in a failed surface of steel fiber reinforced concrete beams. 9th symposium on high performance concrete: design, verification & utilization. Rotorua, New Zealand, 2011.
- [7] Mueller, T: Untersuchungen zum Biegetragverhalten von Stahlfaserbeton und betonstahlbewehrtem Stahlfaserbeton unter Berücksichtigung des Einflusses von Stahlfaserart und Betonzusammensetzung, PhD Thesis. University Leipzig 2013 (in German).